JOURNAL OF BACTERIOLOGY, May 2006, p. 3371–3381 Vol. 188, No. 9
0021-9193/06/$08.00+0 doi:10.1128/JB.188.9.3371–3381.2006

Effect of Chromate Stress on *Escherichia coli* K-12

D. F. Ackerley,[1,2] Y. Barak,[1] S. V. Lynch,[1] J. Curtin,[3] and A. Matin[1]*

Department of Microbiology and Immunology, Sherman Fairchild Science Building, Stanford University School of Medicine, 299 Campus Drive, Stanford, California 94305[1]; School of Biological Sciences, Victoria University of Wellington, PO Box 600, Wellington, New Zealand[2]; and Centers for Disease Control and Prevention, Atlanta, Georgia 30333[3]

Received 15 December 2005/Accepted 19 February 2006

The nature of the stress experienced by *Escherichia coli* K-12 exposed to chromate, and mechanisms that may enable cells to withstand this stress, were examined. Cells that had been preadapted by overnight growth in the presence of chromate were less stressed than nonadapted controls. Within 3 h of chromate exposure, the latter ceased growth and exhibited extreme filamentous morphology; by 5 h there was partial recovery with restoration of relatively normal cell morphology. In contrast, preadapted cells were less drastically affected in their morphology and growth. Cellular oxidative stress, as monitored by use of an H_2O_2-responsive fluorescent dye, was most severe in the nonadapted cells at 3 h postinoculation, lower in the partially recovered cells at 5 h postinoculation, and lower still in the preadapted cells. Chromate exposure depleted cellular levels of reduced glutathione and other free thiols to a greater extent in nonadapted than preadapted cells. In both cell types, the SOS response was activated, and levels of proteins such as SodB and CysK, which can counter oxidative stress, were increased. Some mutants missing antioxidant proteins (SodB, CysK, YieF, or KatE) were more sensitive to chromate. Thus, oxidative stress plays a major role in chromate toxicity in vivo, and cellular defense against this toxicity involves activation of antioxidant mechanisms. As bacterial chromate bioremediation is limited by the toxicity of chromate, minimizing oxidative stress during bacterial chromate reduction and bolstering the capacity of these organisms to deal with this stress will improve their effectiveness in chromate bioremediation.

Chromate [Cr(VI)] is a widespread environmental pollutant, as it is a by-product of numerous industrial processes and nuclear weapons production (5). Because chromate is soluble, environmental contamination is difficult to contain. This solubility also promotes the active transport of chromate across biological membranes (7), and once internalized by cells, Cr(VI) exhibits a variety of toxic, mutagenic, and carcinogenic effects (34, 44). In contrast, most cells are impermeable to Cr(III), which is insoluble under typical environmental conditions (30); as measured by the Ames test, it is therefore some 1,000-fold less mutagenic than Cr(VI) (19). Thus, strategies for decontamination of environmental chromate focus on reducing it to Cr(III). Chemical methods for this are prohibitively expensive for large-scale environmental application and frequently have damaging consequences of their own (7), and so bacterial bioremediation is of considerable interest as an environmentally friendly and affordable solution to chromate pollution.

Several bacteria, including *Escherichia coli*, *Shewanella oneidensis*, and numerous species of *Pseudomonas* and *Bacillus*, can reduce Cr(VI) to Cr(III) (17, 39); nonetheless, an effective bacterial system for in situ reduction has not yet been developed. One reason is that chromate is also toxic to the remediating bacteria (17). Our in vitro studies have strongly implicated oxidative stress generated by chromate as a major cause of this toxicity (1, 2, 3). A wide range of bacterial enzymes and other cellular constituents reduce Cr(VI) by one-electron reduction, generating the highly reactive radical Cr(V), which redox cycles (2, 13, 16, 33). In this process, Cr(V) is oxidized back to Cr(VI), giving its electron to molecular oxygen and generating reactive oxygen species (ROS). Repetition of this process produces large quantities of ROS, subjecting the cells to severe oxidative stress. Our proposed strategy to improve bacterial capacity to remediate chromate is therefore based on minimizing ROS production during chromate reduction. This approach envisages enhancing the efficacy of enzymes which catalyze primarily a one-step transformation of Cr(VI) to Cr(III), avoiding generation of Cr(V) (1, 2; Y. Barak, D. F. Ackerley, B. Lal, and A. Matin, unpublished data).

However, the prooxidant effect of chromate in bacteria has not been demonstrated in vivo, and since countering it is central to our strategy for improving bacterial chromate remediation, we have now examined the effects of chromate at the cellular level in *E. coli*. We observed that chromate exposure induced aberrant cell morphology and other effects and that these effects were markedly altered in cells that had been preadapted to chromate. As these effects were the result of physiological changes, they afforded a good experimental system to gain insight into these changes and determine the role of the potential prooxidant effect of chromate in vivo.

MATERIALS AND METHODS

Bacterial strains and growth conditions. The *E. coli* K-12 strains that were used in this study are listed in Table 1. For growth of these strains as unchallenged, challenged nonadapted, and challenged preadapted cultures, a single colony was inoculated into 5 ml Luria broth (LB) and grown with aeration at 37°C for 8 to 10 h (to an A_{660} of at least 2.5). Fifty-microliter aliquots of this culture were then used to inoculate three fresh cultures in 20-ml test tubes: one containing 5 ml of unamended LB, one containing 5 ml of LB plus 250 μM K_2CrO_4, and one containing 10 ml of LB plus 250 μM K_2CrO_4. Following 14 h of overnight growth (with aeration at 37°C) the A_{660} of each culture was measured. Typically, the A_{660} of the 5-ml chromate-amended overnight culture was

* Corresponding author. Mailing address: Department of Microbiology and Immunology, Sherman Fairchild Science Building, Stanford University School of Medicine, 299 Campus Drive, Stanford, CA 94305. Phone: (650) 725-4745. Fax: (650) 725-6757. E-mail: a.matin@stanford.edu.

TABLE 1. Strains

Strain	Relevant characteristics	Reference or source
AMS6	K-12 *lacU169* F^- λ^-	Lab strain (Stanford isolate)
AB1157	K-12 *thr-1 leu-6 thi-1 lacY1 galK2 ara-14 xyl-5 mtl-1 proA2 his-4 argE3 str-31 tsx-33 supE44 rec*$^+$	From James Imlay (reference 15)
sodA mutant	AB1157 *sodA* mutant (PN132; *sodA*::MudPR13)	15
sodB mutant	AB1157 *sodB* mutant (JI130; *sodB-kan*); Km^r	15
sodAB mutant	AB1157 *sodAB* double mutant as above (JI131); Km^r	15
W3110	K-12 F^- λ^- IN(*rrnD-rrnE*)*1*	Keio collection[a]
cysK mutant	W3110 *cysK* mutant	Keio collection
cysN mutant	W3110 *cysN* mutant	Keio collection
katE mutant	W3110 *katE* mutant	Keio collection
katG mutant	W3110 *katG* mutant	Keio collection
gshA mutant	W3110 *gshA* mutant	Keio collection
gshB mutant	W3110 *gshB* mutant	Keio collection
sodA mutant	W3110 *sodA* mutant	Keio collection
sodB mutant	W3110 *sodB* mutant	Keio collection
yieF mutant	W3110 *yieF* mutant	Keio collection
fliC mutant	W3110 *fliC* mutant	Keio collection
ompW mutant	W3110 *ompW* mutant	Keio collection
ftnA mutant	W3110 *ftnA* mutant	Keio collection
sspA mutant	W3110 *sspA* mutant	Keio collection
MG1655	K-12 F^- λ^- *ilvG rfb-50 rph-1* (CF1648)	From Mike Cashel (reference 43)
relA spoT mutant	MG1655 *relA spoT* mutant (CF1693); Km^r Cm^r	43
pexB::*lacZ* strain	AMS6 single-copy *pexB*::*lacZ* fusion	20
sfiA::*lacZ* strain	K-12 single-copy *sfiA*::*lacZ* fusion	From Stanley Cohen (reference 25)

[a] The URL for the Keio collection is http://ecoli.aist-nara.ac.jp/gb5/Resources/deletion/deletion.html.

between 2.0 and 2.5: if so, this was used as the inoculum for the challenged preadapted culture; if not, the 10-ml chromate-amended overnight culture was used, provided its A_{660} was between 2.0 and 2.5. The overnight culture grown in unamended LB was used to inoculate both the unchallenged and the challenged nonadapted cultures. Unchallenged, challenged nonadapted, and challenged preadapted cultures were grown from a starting A_{660} of 0.1 in 20 ml LB containing 250 μM K_2CrO_4 as appropriate, at 37°C with aeration, in 50-ml unbaffled flasks.

Assays. For shaken-flask growth assays, A_{660} was measured using a Shimadzu temperature-controlled UV/visible spectrophotometer, with cultures diluted 1/10 in LB to measure A_{660}s of >1. MIC_{50} (defined as the lowest concentration of chromate required to reduce cell growth in a microtiter plate well by 50% relative to the unexposed control) assays were conducted in the innermost 60 wells of 96-well plates, the outer wells being filled with 250 μl H_2O to minimize evaporation. Triplicate 10-well series of 200-μl LB aliquots containing increasing concentrations of K_2CrO_4 were inoculated to a starting A_{660} of 0.1 for each strain. An increasing series of 0 to 450 μM chromate with 50 μM increments was used for all strains except those from the Keio collection, which were more resistant; with the Keio strains, 0, 100, 200, 250, 300, 350, 400, 500, 600, and 700 μM concentrations were used. Plates were grown with shaking at 37°C for 8 h, after which the H_2O in one of the outer wells was replaced with 200 μl LB as a blank, and the A_{660} for each well was read in a BioTek microplate S330 plate reader.

Reduced glutathione and total cell thiol measurements were made using a glutathione assay kit (Calbiochem, San Diego, CA). Protein concentrations were measured with a Bio-Rad Dc protein assay kit using bovine serum albumin as the standard. Whole-cell chromate reduction assays were performed as previously described (2) except that they were normalized against protein concentration rather than A_{660}. Cells from each culture were resuspended to a final protein concentration of 7.5 mg · ml^{-1} in LB containing 400 μM K_2CrO_4 (equivalent to a final A_{660} of around 8.0 for the unchallenged cells) and incubated with aeration at 37°C for 1 h, with residual chromate being measured by the diphenyl carbazide method (2) every 10 min. β-Galactosidase activity was measured as previously described (20) except that activity was normalized against cellular protein concentration rather than A_{660}, with 1 Miller Unit (MU) defined as ΔA_{574}/min/mg protein. Thin-layer chromatography ppGpp assays were conducted as described previously (40).

2D-PAGE. Two-dimensional polyacrylamide gel electrophoresis (2D-PAGE) was performed according to the method of O'Farrell (27) by Kendrick Labs, Inc. (Madison, WI). Samples (5.0 ml/culture A_{660}) were collected from unchallenged, challenged nonadapted, and challenged preadapted cultures of *E. coli* strain AMS6 at 3 h and 5 h postinoculation. Cells were pelleted by centrifugation, and protein samples were prepared by addition of 300 μl osmotic lysis buffer (Kendrick Labs, Inc.) containing 10× protease inhibitor and nuclease stock. One hundred microliters of sodium dodecyl sulfate (SDS) boiling buffer minus β-mercaptoethanol was added to each sample, and samples were boiled for 5 min, after which protein concentrations were estimated using a bicinchoninic acid assay (Pierce Chemical Co., Rockford, IL). Samples were then lyophilized, redissolved to 6 mg · ml^{-1} protein in SDS boiling buffer, and heated in a boiling water bath for 3 min prior to loading. Isoelectric focusing was carried out in 3.5-mm-inner-diameter glass tubes using 2% (wt/vol) pH 4 to 8 ampholines (Gallard-Schlesinger Industries, Inc., Garden City, NY) for 20,000 V · h. Fifty nanograms of an isoelectric focusing internal standard, tropomyosin, was added to each sample prior to loading, giving two polypeptide spots with similar pIs; the lower spot, with a molecular weight of 33,000 and pI 5.2, is marked with an arrow on each 2D gel image. After reaching equilibrium in SDS sample buffer (10% [wt/vol] glycerol, 50 mM dithiothreitol, 2.3% [wt/vol] SDS, and 62.5 mM Tris, pH 6.8), each tube gel was sealed to the top of a stacking gel overlaying a 10% (wt/vol) acrylamide slab gel (0.75 mm thick). SDS slab gel electrophoresis was carried out for 5 h at 25 mA/gel. Molecular mass standards were added to the agarose that sealed the tube gel to the slab gel, and these standards appear as horizontal lines on the Coomassie blue-stained 10% acrylamide slab gels. Gels were dried between sheets of cellophane paper with the acid edge to the left.

Analysis of spots on 2D-PAGE gels. Gel analysis was performed by Kendrick Labs, Inc. (Madison, WI). Duplicate gels were obtained as described above, and one gel from each pair was scanned with a laser densitometer (model PDSI; Molecular Dynamics Inc., Sunnyvale, CA). The scanner was checked for linearity prior to scanning with a calibrated neutral-density filter set (Melles Griot, Irvine, CA). The images were analyzed using Nonlinear Technology Progenesis software (version 2003.03) such that all major spots and all changing spots were outlined, quantified, and matched on all the gels. The general method of computerized analysis for these pairs included automatic spot finding and quantification, automatic background subtraction (Progenesis algorithm), and automatic spot matching in conjunction with detailed manual checking of the spot-finding and -matching functions. The spot intensities on each gel were expressed as a percentage of the total density of all spots on the gel and averaged between duplicate gels. These values were then compared for equivalent spots on different gels, with threefold or greater differences in intensity regarded as significant up- or down-regulation of individual proteins. Twenty clearly delineated spots whose intensity was significantly altered were excised and sent to the Protein Chemistry Core Facility of Columbia University for matrix-assisted laser desorption ionization mass spectrometry (MALDI-MS) fingerprinting; of these, 18 were success-

TABLE 2. Changes in protein expression: challenged nonadapted versus unchallenged cells

Growth time and spot no.	Protein[a]	Gene	Expression change[b]	Known or suspected function
3 h				
1	Flagellin	*fliC*	11-fold down	Flagellar subunit
2	ADP-L-glycero-D-manno-heptose-6-epimerase	*hldD*	4.1-fold down	Lipopolysaccharide biosynthesis
5 h				
3	Superoxide dismutase (ferric; chain B)	*sodB*	+++	Decomposition of $O_2 \cdot^-$
4	Sulfate adenylyl transferase	*cysN*	6.3-fold up	Cysteine biosynthesis
5	Cysteine synthase A	*cysK*	4.1-fold up	Cysteine biosynthesis
1	Flagellin	*fliC*	—	Flagellar subunit
2	ADP-L-glycero-D-manno-heptose-6-epimerase	*hldD*	3.8-fold down	Lipopolysaccharide biosynthesis
6	Cytoplasmic ferritin	*ftnA*	3.8-fold down	Iron storage
7	Putative formate acetyl transferase	*yfiD*	3.3-fold down	Unknown

[a] The proteins in spots 3, 4, and 5 were up-regulated by chromate challenge; all other proteins in the table were down-regulated by chromate.
[b] +++ indicates a spot detected only on the challenged nonadapted gel; — indicates a spot detected only on the unchallenged gel.

fully identified. For each of these, the measured molecular mass and pI were consistent with those calculated from sequence data (NCBI databases; http://www4.ncbi.nlm.nih.gov/entrez/query.fcgi) using PeptideMass (http://us.expasy.org/tools/peptide-mass.html). Protein functions were annotated for Tables 2 and 3 with assistance from EcoCyc databases (http://ecocyc.org/).

Scanning electron microscopy. Samples (5 ml) were collected from unchallenged, challenged nonadapted, and challenged preadapted cultures at 3 h and 5 h postinoculation and fixed by addition of 5 ml of 2% glutaraldehyde in 10 mM Tris-HCl (pH 7.5). The cells were centrifuged at 4,000 × *g* for 15 min and resuspended in 5 ml of 10 mM phosphate-buffered saline (PBS; pH 7.0). Aliquots of 1 ml of each resuspended sample were passed through a 0.1-μm membrane filter (Nuclepore, CA) and the filters dehydrated through a series of aqueous ethanol (30 to 100%) for durations of 10 to 15 min. Specimen filters were subsequently immersed in hexamethyldisilazane (Polysciences Inc., PA) and allowed to dry overnight at room temperature. Samples were mounted on aluminum stubs with quick-drying silver paint (Ted Pella Inc., CA), coated in gold (Polaron SC7640 Sputter Coater; Thermo VG Scientific, United Kingdom), and viewed and photographed with a Philips XL30 ESEM scanning electron microscope.

Fluorescence microscopy. Samples (0.5 ml/culture A_{660}) were collected from unchallenged, challenged nonadapted, and challenged preadapted cultures at 3 h and 5 h postinoculation, pelleted by centrifugation, washed once in PBS, resuspended in LB containing 30 μM 2′, 7′-dihydrodichlorofluorescein diacetate (H_2DCFDA), and incubated in the dark with rotation for 10 min at 37°C. Each sample was then pelleted by centrifugation, washed once in PBS, repelleted, and resuspended in 50 μl PBS. Five microliters was spotted onto a glass microscope slide and allowed to air dry in the dark. Five microliters of Vectashield (Vector Inc., CA) fluorescence antiquenching mounting medium was spotted on top of the air-dried sample and covered with a glass coverslip. Samples were visualized at 1,000× magnification on an Olympus BX60 upright fluorescence microscope, and black-and-white images were captured with a Hamamatsu Orca100 charge-coupled device through a green filter and pseudocolored with identical settings for each image using Image Pro Plus 5.0.

RESULTS

Chromate has a marked effect on cell morphology and growth kinetics. Unless otherwise stated, the K_2CrO_4 concentration used was 250 μM. In chromate-amended LB medium,

TABLE 3. Changes in protein expression: challenged preadapted versus challenged nonadapted cells

Growth time and spot no.	Protein[a]	Gene	Expression change[b]	Known or suspected function
3 h				
8	Alkane sulfonate monooxygenase	*ssuD*	+++	Conversion of alkane sulfonates to aldehyde plus sulfite; induced by sulfur limitation
9	Stringent starvation protein A	*sspA*	+++	Starvation/stress response; indirect +ve regulator of σ^s (by −ve regulation H-NS)
10	Pyruvate dehydrogenase	*aceF*	4.9-fold up	Intermediary metabolism
11	Glycyl-tRNA synthetase (β-chain)	*glyS*	3.4-fold up	Protein synthesis
12	Trehalose-6-phosphate hydrolase	*treC*	3.3-fold up	Trehalose degradation; down-regulated by osmotic stress
13	Outer membrane protein W	*ompW*	—	Colicin receptor; putative general stress response protein
14	Uncharacterized; glycolate operon	*glcG*	—	Unknown; suspected antioxidant protein
15	Carbamoyl-phosphate synthase A	*carA*	6.1-fold down	Carbamoyl phosphate (precursor of arginine and pyrimidines) synthesis
16	Periplasmic dipeptide transport protein	*dppA*	4.8-fold down	Dipeptide transport; starvation stress
5 h				
1	Flagellin	*fliC*	+++	Flagellar subunit
8	Alkane sulfonate monooxygenase	*ssuD*	+++	Conversion of alkane sulfonates to aldehyde plus sulfite; induced by sulfur limitation
17	Malate synthase A	*aceB*	5.4-fold up	Intermediary metabolism
13	Outer membrane protein W	*ompW*	—	Colicin receptor; putative general stress response protein
18	Outer membrane protein A	*ompA*	3.8-fold down	Colicin receptor; down-regulated by starvation

[a] The proteins in spots 8, 9, 10, 11, and 12 for cells grown for 3 h and spots 1, 8, and 17 for cells grown for 5 h were up-regulated by preadaptation. All other proteins in the table were down-regulated by preadaptation.
[b] +++ indicates a spot detected only on the challenged preadapted gel; — indicates a spot detected only on the challenged nonadapted gel.

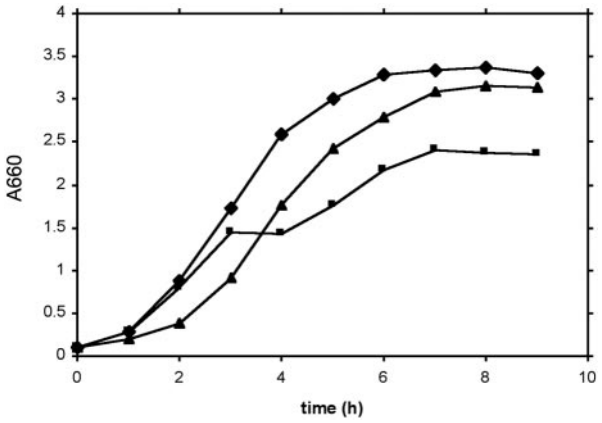

FIG. 1. Growth kinetics (A_{660}) for unchallenged (◆), challenged nonadapted (■), and challenged preadapted (▲) cells inoculated at an initial A_{660} of 0.1 into flask cultures of LB with or without 250 μM K_2CrO_4, as appropriate, and grown at 37°C with shaking.

E. coli exhibited biphasic growth kinetics, as measured by changes in A_{660}. For the first 3 h, growth occurred at almost the same rate as in LB medium without chromate (Fig. 1). A temporary lag then ensued, with growth resuming, but more slowly, by around 5 h postinoculation. The final A_{660} in the chromate-containing medium was considerably lower than in unamended LB. Chromate preadaptation dramatically altered these kinetics. When cells that had been grown overnight (14 h) in chromate-LB medium were used to inoculate fresh chromate-containing LB, their growth kinetics were similar to the unchallenged cells. Although a longer lag phase was seen, the subsequent growth rate and final A_{660} resembled the control LB culture (Fig. 1). For convenience, we will refer to these three types of cultures, or cell types, as "unchallenged," "challenged nonadapted," and "challenged preadapted."

The reversion of the preadapted cells to growth kinetics resembling the unchallenged cells could have been due to the selection of chromate-resistant mutants. However, when cells from the challenged preadapted culture were grown overnight in unamended LB medium and then used to inoculate fresh chromate-containing LB medium, the resulting culture lost the preadaptation response and displayed challenged nonadapted growth kinetics (i.e., biphasic, as in Fig. 1). Thus, like the response of the nonadapted cells to chromate exposure, the challenged preadapted growth phenotype is the result of changes in cellular physiology. To gain an insight into these changes, we decided to compare a number of parameters in the different cell types at the 3- and 5-h postinoculation time points.

Phase-contrast microscopy indicated changes in cell size upon chromate challenge, and to examine this more closely, we visualized unchallenged, challenged nonadapted, and challenged preadapted cells with a scanning electron microscope (5,000-fold magnification). At both 3- and 5-h time points, the unchallenged cells were small rods (ca. 1 to 2 by 0.5 μm) (Fig. 2A and B). In contrast, the challenged nonadapted cells grown for 3 h (3-h challenged nonadapted cells), although retaining about the same width, were greatly elongated (up to 50 μm in length) (Fig. 2C). By 5 h postinoculation, the extreme snake-like forms had disappeared, but the cells remained relatively long (2 to 5 μm) (Fig. 2D). Less dramatic morphological changes were seen upon fresh chromate challenge of the preadapted cells. Although at 3 h postinoculation they exhibited typical lengths of 4 to 6 μm (Fig. 2E), by 5 h they were only slightly more elongated than the unchallenged cells (Fig. 2F).

As these dramatic changes in size may have resulted in A_{660} measurements (Fig. 1) not accurately reflecting cell growth, growth was instead monitored by cellular protein measurement for the three conditions. The increase in cell protein versus time plot (Fig. 2G) shows that biomass increase does not occur in the challenged nonadapted culture after about 3 h and that the increase in A_{660} seen in Fig. 1 after this time point resulted from fragmentation of the snake forms. However, the increased lag in growth caused by chromate challenge of preadapted cells is still seen.

Given the dramatic changes in these parameters, we wondered if they affected the chromate transformation capacity of the bacteria. Dense cell suspensions, containing 7.5 mg cell protein ml^{-1} in LB medium amended with 400 μM K_2CrO_4, were used to explore this (as in reference 2). At all time points examined (3, 5, and 7 h), the unchallenged, challenged nonadapted, and challenged preadapted cells exhibited similar rates of chromate transformation and a parallel decline in this rate with continued incubation (Table 4).

Prooxidant effect of chromate in vivo. The above results suggest that nonadapted cells exposed to chromate are initially able to withstand its effect but by about 3 h postinoculation undergo cell growth arrest and then are able to partially recover at around 5 h postinoculation in terms of regaining more normal cell morphology. In contrast, the preadapted cells undergo physiological changes that enhance their capacity to withstand the chromate stress. Thus, chromate exposure sets into motion remedial measures, and if these are concerned with countering the prooxidant effect of chromate, as we suspect, then the unchallenged, challenged nonadapted, and challenged preadapted cells should exhibit different levels of oxidative stress.

To test this notion, we collected culture samples at 3 and 5 h, treated them with the ROS-activated green fluorescent dye H_2DCFDA, and examined them at 1,000× magnification with an Olympus BX60 upright fluorescence microscope. Unchallenged cells were the least fluorescent at both time points (Fig. 3A and B), while the 3-h nonadapted challenged cells exhibited the greatest fluorescent intensity (Fig. 3C), this being somewhat reduced at the 5-h postinoculation time point (Fig. 3D). In the preadapted cells, the fluorescence was less at both time points than in the nonadapted challenged cells, and the 5-h cells again exhibited less intensity than the 3-h cells (Fig. 3E and F).

We hypothesized that if chromate exerts oxidative stress in vivo, as indicated by the above results, this should be further reflected in its effect on cellular antioxidant metabolites. The tripeptide glutathione (GSH) and other thiols are major cellular antioxidants (6), and we measured their levels in the different cell types. In unchallenged cells, GSH and total free thiol concentrations rose as the cells progressed through exponential into the stationary phase (Fig. 4). In both challenged nonadapted and challenged preadapted cells, however, chromate exposure brought about an immediate decline in the levels of these metabolites, and it was not until around the 5-h

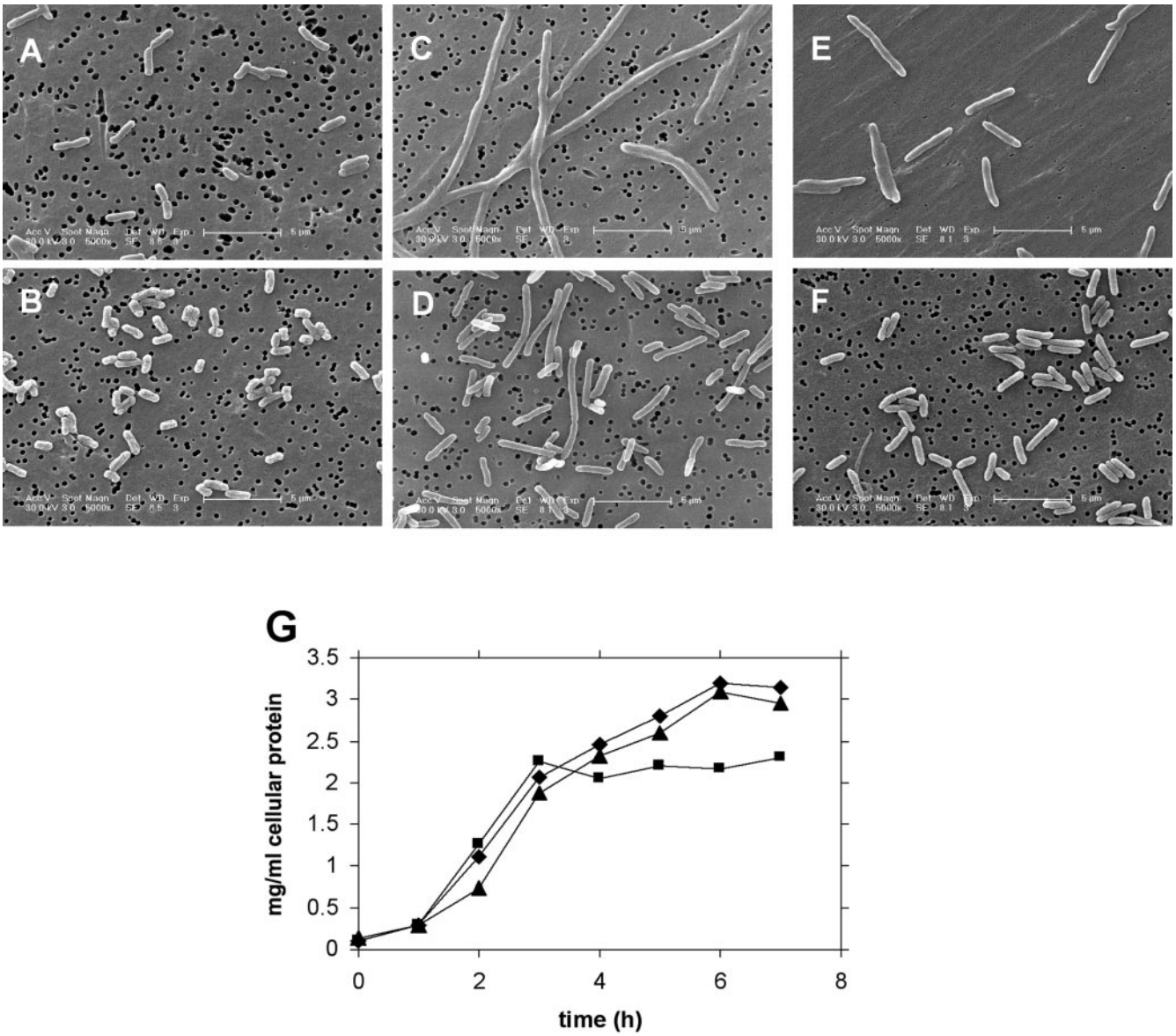

FIG. 2. Representative scanning electron micrographs (5,000× magnification) of cells from unchallenged (A, 3 h postinoculation; B, 5 h postinoculation), challenged nonadapted (C, 3 h postinoculation; D, 5 h postinoculation), and challenged preadapted (E, 3 h postinoculation; F, 5 h postinoculation) cultures. In all figures, the scale bar indicates 5 μm. (G) Cellular protein concentration (mg · ml^{-1}) of samples collected from unchallenged (◆), challenged nonadapted (■), and challenged preadapted (▲) cultures at hourly intervals.

TABLE 4. Chromate reduction rates[a]

Cell growth time	Time postresuspension (min)	Residual chromate in medium (μM)		
		Unchallenged	Nonadapted	Preadapted
3 h	0	400	400	400
	30	304	309	306
	60	263	264	255
5 h	0	400	400	400
	30	325	318	321
	60	282	276	280
7 h	0	400	400	400
	30	334	337	328
	60	301	296	290

[a] Duplicate independent experiments were conducted. All errors (1 standard deviation) were within ± 4%.

time point that these levels began to recover (Fig. 4). Furthermore, consistent with the fluorescence microscopy results indicating heightened levels of oxidative stress in the challenged nonadapted cells (Fig. 3), free thiol and GSH levels declined more sharply, and to a greater extent, in nonadapted than in preadapted cells (Fig. 4).

To gain further insight into the physiological effects of chromate exposure, we compared the 2D gel pattern of different cell types at the 3-h (Fig. 5A) and 5-h (Fig. 5B) time points. The identities of selected protein spots were also determined, as described in Materials and Methods, and are summarized in Table 2 for challenged nonadapted versus unchallenged cells and Table 3 for challenged preadapted versus challenged nonadapted cells.

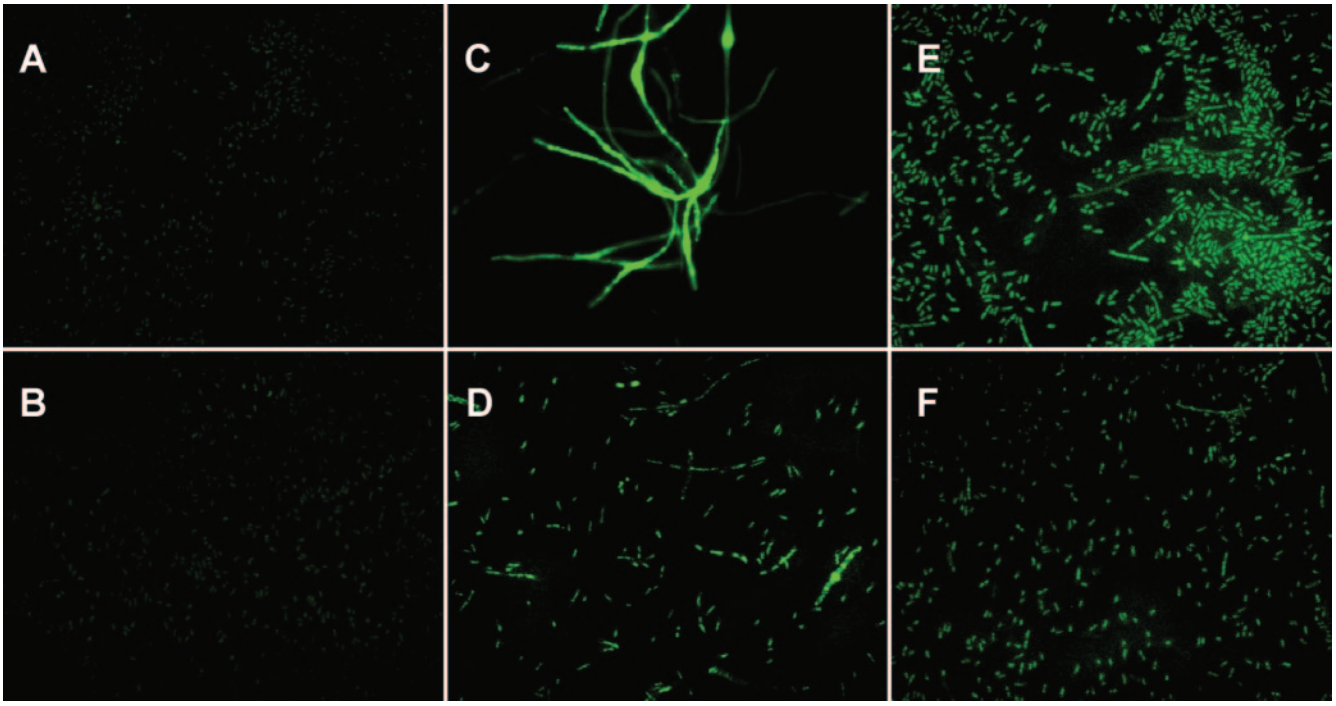

FIG. 3. Representative fluorescent micrographs (1,000× magnification) of cells from unchallenged (A, 3 h postinoculation; B, 5 h postinoculation), challenged nonadapted (C, 3 h postinoculation; D, 5 h postinoculation), and challenged preadapted (E, 3 h postinoculation; F, 5 h postinoculation) cultures treated with the H_2O_2-activated green fluorescent dye H_2DCFDA as described in Materials and Methods. The increased green fluorescence observed in the chromate-challenged cultures is indicative of heightened oxidative stress.

Chromate challenge in nonadapted cells caused down-regulation of two proteins at the 3-h time point (Table 2), neither of which appears to be related to oxidative stress. However, at the 5-h time point this condition resulted in the synthesis or up-regulation of three proteins with potential antioxidant roles, Fe-superoxide dismutase (SodB, decomposition of $O_2 \cdot^-$), sulfate adenylyl transferase, and cysteine synthase (CysN and CysK, respectively, which by contributing to cysteine biosynthesis can augment cellular thiol pools). Each of these enzymes is typically up-regulated in bacteria subjected to oxidative stress (9, 26, 29). It should also be noted that up-regulation of these proteins at the 5-h time point coincides with the partial recovery from chromate stress as reflected by restoration of relatively normal cell morphology (Fig. 2D), reduced cellular oxidative stress as monitored by H_2DCFDA-mediated fluorescence (Fig. 3D), and partial replenishment of cellular thiols (Fig. 4). Four proteins were down-regulated at this time point (Table 2).

Consistent with an active role in cell recovery from chromate stress, CysN and CysK were further up-regulated in chromate-challenged preadapted cells relative to the nonadapted cells, although not beyond our threefold significance criteria (up-regulated 2.24- and 1.86-fold, respectively, at 3 h and 1.35- and 1.15-fold at 5 h). An additional protein, alkane sulfonate monooxygenase, which may have a role in thiol biosynthesis, as it provides a source of sulfur (11), was also induced in chromate-preadapted cells at both the 3-h and 5-h time points (Table 3). Other proteins up- or down-regulated in both types of cells included flagellar synthesis, intermediary metabolism, and various stress-responsive proteins.

The above results provide in vivo evidence of chromate-mediated oxidative stress and suggest that the cell attempts to counter it by inducing antioxidant proteins. It can thus be predicted that mutants missing antioxidant proteins will show greater sensitivity to chromate. We tested this premise by comparing the MIC_{50}s for chromate between a range of isogenic single-gene knockout mutants and the wild type grown in shaken microtiter plate wells, as described in Materials and Methods. Several of the oxidative stress mutants examined displayed a lowered MIC_{50} for chromate relative to their isogenic wild type (Table 5). This was seen for the *katE* catalase mutant; the chromate reductase and putative H_2O_2-quenching quinone reductase *yieF* mutant (1, 12); and two mutants lacking enzymes up-regulated by chromate in the 2D gel analysis, the *cysK* and *sodB* mutants (Fig. 5 and Tables 2 and 3). In contrast, the *katG* catalase mutant, the *cysN* mutant, the *sodA* (manganese) superoxide dismutase mutant, and interestingly, given the results presented in Fig. 4B, the glutathione biosynthesis mutants *gshA* and *gshB* did not have reduced chromate MIC_{50}s. The *sodA* mutant MIC_{50} in fact appeared to be slightly increased, but in different *E. coli* K-12 mutants (strain AB1157; Table 1), we did not observe this. Wild-type AB1157 and its isogenic *sodA* and *sodB* mutants all displayed an MIC_{50} for chromate of 250 μM, but the isogenic *sodAB* double mutant exhibited an MIC_{50} of 150 μM. The latter results suggest a protective role for both SodA and SodB and also emphasize that there is likely to be some functional redundancy between different antioxidant enzymes, buffering the effect of individual knockout mutations on MIC_{50}s.

Mutants lacking some of the other proteins whose expres-

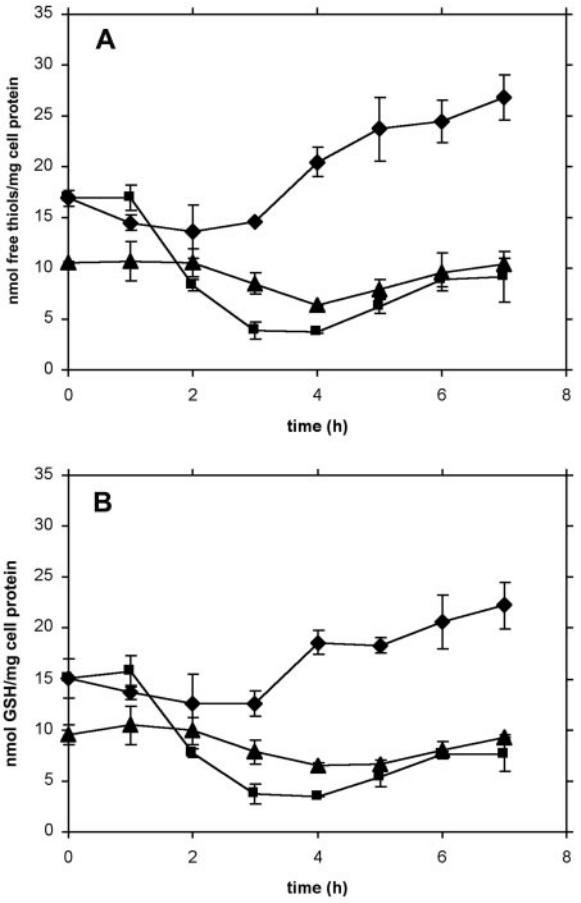

FIG. 4. Total free thiol (A) and reduced glutathione (B) levels in cells collected from unchallenged (◆), challenged nonadapted (■), and challenged preadapted (▲) cultures at hourly intervals. Results are the means of two independent measurements, and error bars indicate ±1 standard error of the mean.

sion was altered on the 2D gels (*ftnA*, *fliC*, *ompW*, and *sspA*) did not exhibit reduced chromate MIC_{50}s.

Does chromate activate global stress responses? Various cellular insults activate global stress responses. The SOS response in *E. coli* is known to be activated by oxidative stress (15) and to promote cell filamentation (10) and thus appeared to be a likely candidate for activation by chromate. To investigate this possibility, we examined β-galactosidase activity in an SOS-regulated single-copy *sfiA*::*lacZ* fusion strain (Table 1) (25) in the different chromate stress conditions. In unchallenged cells we saw no significant β-galactosidase induction (Fig. 6A), while in chromate-challenged, nonadapted cells we observed gradual induction, culminating in about a 10-fold increase in activity at 5 h, after growth of this strain had ceased (Fig. 6A and 2G). In contrast, the chromate-challenged preadapted cells exhibited relatively high levels of β-galactosidase activity initially (approximately fivefold that of the unchallenged and challenged nonadapted cells at time zero), and these levels remained mostly constant throughout the rest of the growth period. The data suggest that the SOS response induced during the adaptive period may play a role in the ability of the preadapted cells to better withstand chromate-induced oxidative stress. Expression of several other *E. coli* SOS genes has previously been shown to be induced by Cr(VI) compounds (18).

The proteomic analysis indicated induction of several stress- and starvation-related genes, and this prompted us to also investigate the involvement of σ^s and ppGpp in the chromate stress response. The former is the central regulator of the bacterial general stress response (23, 28) and the latter that of the stringent response (22), and increases in their concentrations signal the activation of these responses. As indicated by use of the *pexB*::*lacZ* transcriptional fusion strain (Table 1), whose β-galactosidase activity is a reliable measure of σ^s levels (21), not only does chromate stress not induce σ^s activity directly, it also seems to reduce the basal activity that is normally stimulated by starvation and other stationary-phase conditions (Fig. 6B). We also found no increase in levels of ppGpp in chromate-stressed cells, nor were the MIC_{50} or growth kinetics in the presence of chromate affected in a *relA spoT* (ppGpp null) (Table 1) (43) mutant relative to the wild type (not shown). These results suggest the absence of activation of either of these mechanisms in chromate-challenged cells.

DISCUSSION

This study was undertaken to determine the nature of stress that chromate exerts in bacteria in vivo and to gain insight into mechanisms that may enable cells to counter it. The different degrees of sensitivity to chromate exhibited by the non- and preadapted cells occurred without an altered rate of chromate transformation and thus did not involve avoidance of chromate, as might occur by insulating the cell against chromate transport. Instead, they reflected adaptations to withstand the cellular consequences of chromate stress and thus offered an excellent experimental system to address the queries of this study.

Nonadapted chromate-challenged cells were the most stressed. Although in terms of growth kinetics they appeared largely unaffected for the first 3 h postinoculation, by that point they had transitioned to an extreme filamentous morphology, and growth apparently ceased thereafter. By 5 h postinoculation, although growth was not resumed, these cells had regained relatively normal morphologies, indicating partial recovery from chromate stress. Cells preadapted to chromate by overnight incubation in its presence exhibited less severe signs of stress when subjected to fresh chromate challenge. Their cell morphology was altered much less dramatically, and their growth defects were confined to a longer lag phase and slightly lower final cell biomass.

Control cells not challenged with chromate showed little internal oxidative stress according to the degree of green fluorescence they exhibited when incubated with the dye H_2DCFDA. In the chromate-challenged cells, the fluorescence intensity corresponded by and large with the severity of chromate stress noted above. Thus, the 3-h nonadapted cells generated the most intense fluorescence, which declined at 5 h postinoculation coincident with partial recovery, and the preadapted cells, although more fluorescent than the controls, exhibited less internal oxidative stress at both the 3-h and 5-h time points than the challenged nonadapted cells.

Chromate exposure also resulted in depletion of cellular

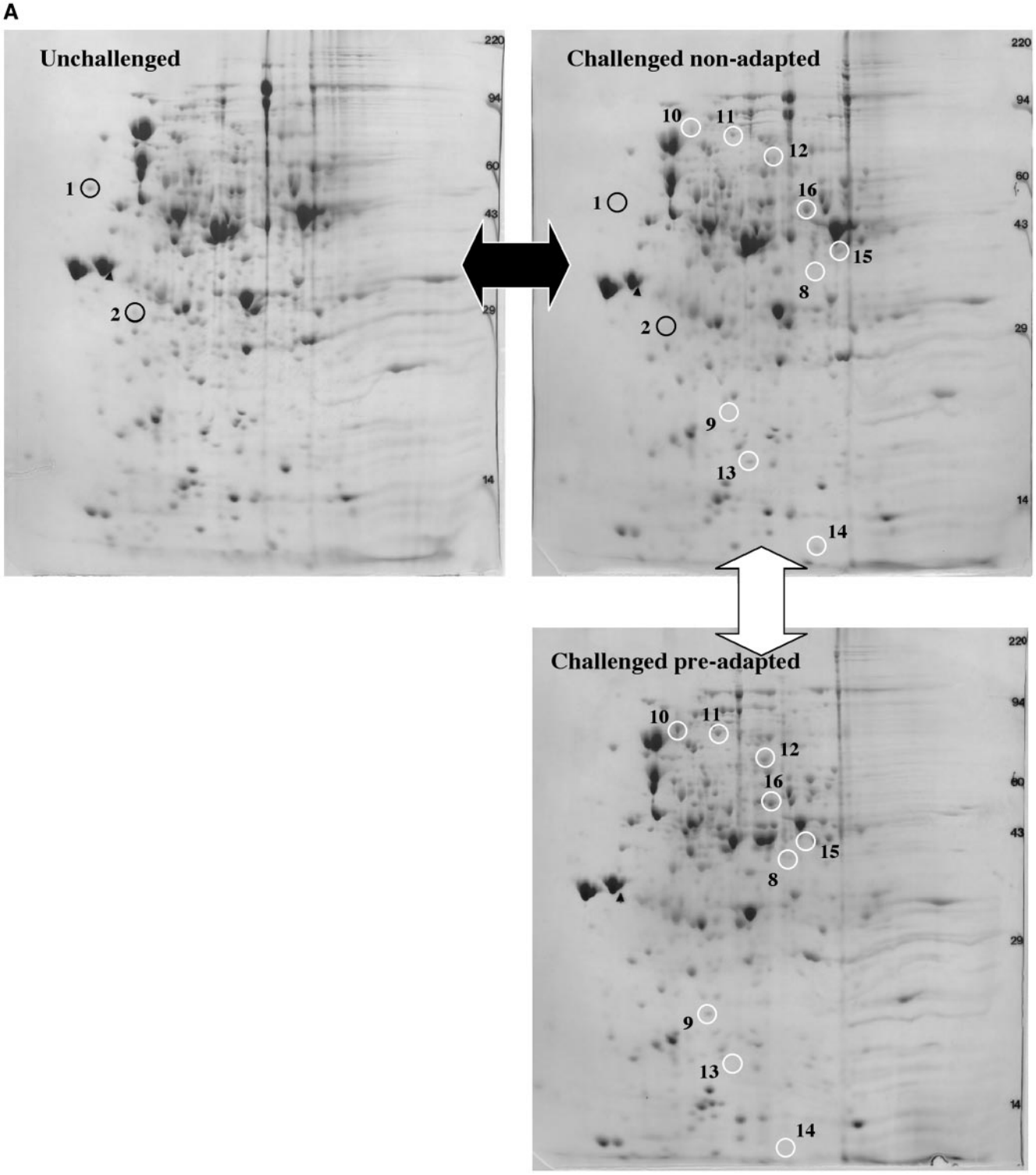

FIG. 5. Coomassie-stained two-dimensional polyacrylamide gels of total cellular protein samples collected from unchallenged, challenged nonadapted, and challenged preadapted cultures 3 h (A) and 5 h (B) postinoculation. Average spot densities from duplicate gels were compared for the unchallenged and challenged nonadapted samples (indicated by the black two-way arrows) and for the challenged nonadapted and challenged preadapted samples (indicated by the white two-way arrows). Distinct protein spots whose expression was up- or down-regulated threefold or greater (ringed in black for the unchallenged versus challenged comparison and in white for the nonadapted versus preadapted comparison) were excised and identified by MALDI-MS fingerprinting. The expression change (*n*-fold) and identities of these proteins are listed in Tables 2 and 3. The black triangle on each gel indicates the internal tropomyosin standard (molecular weight of 33,000; pI 5.2).

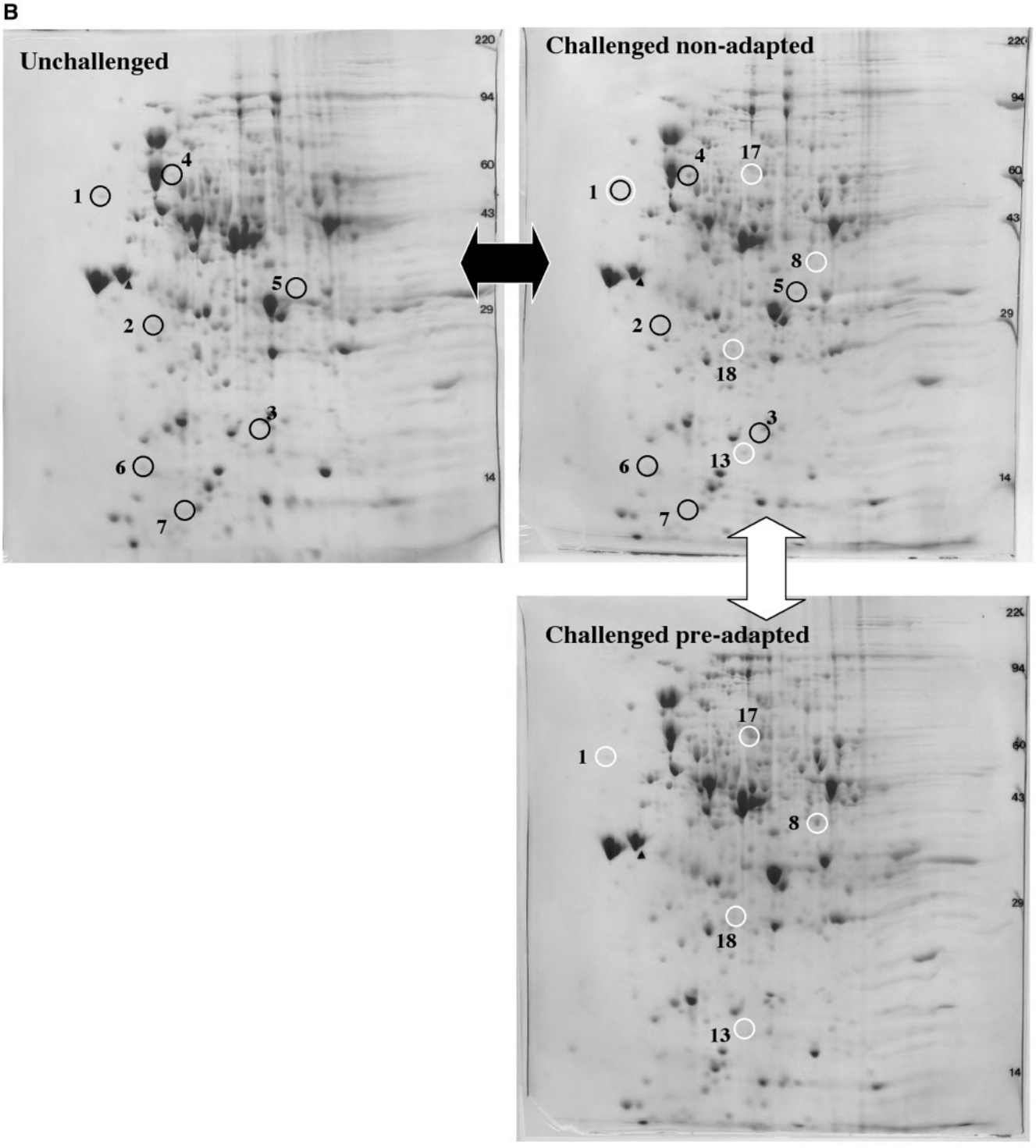

FIG. 5—*Continued*.

GSH and other free thiols, with levels declining more rapidly, and to a greater extent, in nonadapted than preadapted cells. Levels of these metabolites began to be replenished coincident with reduction in internal oxidative stress and cellular recovery as noted above. These events also coincided with the induction of proteins likely to be involved in countering the oxidative stress: SodB, CysN, and CysK (the latter enzyme having also been found to provide *E. coli* with resistance to the heavy metal prooxidant tellurite [36]). Mutants missing some antioxidant defense proteins, such as those encoded by *sodB*, *cysK*, and *katE*, exhibited increased sensitivity to chromate. And the SOS response, which protects against oxidative stress, was activated

TABLE 5. MIC_{50}s of *E. coli* W3110 mutants defective in known genes of antioxidant defense or encoding proteins whose expression was altered on the 2D gels pictured in Fig. 5A and B

Strain	Chromate MIC_{50} (μM)
Wild type	400
cysK mutant[a,b]	300
cysN mutant[a,b]	400
sodA mutant[b]	450
sodB mutant[a,b]	350
katE mutant[b]	300
katG mutant[b]	400
gshA mutant[b]	400
gshB mutant[b]	400
yieF mutant[b]	300
fliC mutant[a]	400
ompW mutant[a]	450
ftnA mutant[a]	400
sspA mutant[a]	400

[a] The proteins encoded by the missing gene had altered expression profiles on 2D gels.
[b] These are oxidative stress mutants.

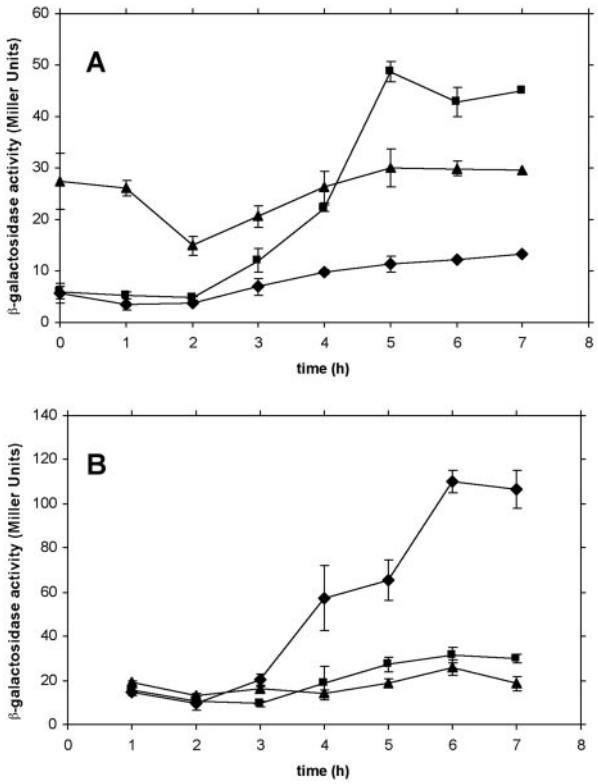

FIG. 6. β-Galactosidase activity determined during the growth of *sfiA*::*lacZ* (A) and *pexB*::*lacZ* (B) single-copy fusion strains in unchallenged (◆), challenged nonadapted (■), and challenged preadapted (▲) cultures. Results are the means of three experimental replicates, and error bars indicate ±1 standard error of the mean. The zero time values were omitted from panel B, as the very high activity in the unchallenged overnight culture was off scale (these values were the following: unchallenged and challenged nonadapted, 209 ± 15 MU; and challenged preadapted, 136 ± 19 MU).

in preadapted cells. Taken together, the bulk of the data demonstrate that the prooxidant properties of chromate play a major role in its toxicity in vivo and that cellular defense against this toxicity involves activation of antioxidant mechanisms.

Although antioxidant capabilities of reduced glutathione are well established, the *gshA* and *gshB* glutathione biosynthesis mutants were not impaired in chromate MIC_{50}. The reason for this is not known but may be related to the fact that GSH can react directly with chromate to form redox-cycling Cr(V) (32), can increase the incidence of Cr(VI)-induced DNA strand breaks (35), and can lead to formation of glutathione-Cr(III)-DNA adducts (37). Thus, in the context of chromate challenge, whether GSH is of net benefit or liability to a cell is difficult to evaluate, with its usual ability to guard cellular constituents against oxidative stress in conflict with its direct interactions with chromium. Indeed, the lower initial levels of GSH in cells which had been preadapted to chromate (Fig. 4B) may actually have contributed to the lower levels of oxidative stress observed in these cells. Consistent with this, Woods et al. (42) showed that when rat kidney cells were challenged with chromate, cells which had been grown on media enabling them to sustain eightfold normal intracellular GSH levels generated higher levels of ROS, and were less viable, than regular cells. Given these complexities, further work is required to establish any protective role for glutathione in defending against chromate stress.

The expression of several stress-responsive proteins was altered in chromate-preadapted cells (Table 3). These included TreC (trehalose-6-phosphate hydrolase, affected by osmotic stress [8]); OmpA, OmpW, AceF, and DppA (outer membrane proteins A and W, pyruvate dehydrogenase, and periplasmic dipeptide transport protein, respectively, affected by pH, starvation, and other stresses [24, 31, 38, 41]); and SspA (stringent starvation protein A, a starvation, salt, and putative global stress response regulator [14]). Although a coherent pattern for the expression of these diverse stress-responsive proteins was hard to discern, we investigated several candidate stress response systems to see if they might play some part in the chromate preadaptation phenotype. However, apart from the fact that the SOS response is likely induced by chromate, no evidence indicated the activation of these other global stress responses.

Activation of the SOS response can provide resistance to future oxidative challenges (4), and this, together with the diminished initial levels of GSH present in chromate-preadapted cells, may provide an explanation for the increased tolerance of these cells to subsequent chromate challenge. It is clear that chromate challenge places a substantial oxidative burden upon both nonadapted and preadapted cells and therefore that enhancing bacterial ability to minimize ROS generation during chromate reduction, and to deal with oxidative stress, will improve the ability to remediate chromate. Apart from the obligatory two-electron chromate reducers we have previously proposed (1, 2), the present work identifies other antioxidant proteins as possible targets of improvement in this regard.

ACKNOWLEDGMENTS

We are grateful to David Alexander for assistance with fluorescence microscopy; Derek Wells for assistance with the ppGpp assays; Claudio Gonzalez, James Imlay, Mike Cashel, and Stanley Cohen for pro-

viding strains; and Chris Miller for stimulating discussion and useful advice.

This work was supported by grants DE-FG03-97ER-624940, DE-FG02-96ER20228, and DE-FG02-05ER64122 from the Natural and Accelerated Bioremediation Program of the U.S. Department of Energy (to A.M.). D.F.A., Y.B., and S.V.L. were supported, in part, by FRST New Zealand Postdoctoral Fellowship STAX0101, a Lady Davis Postdoctoral Fellowship, and a Stanford Medical School Dean's Fellowship, respectively.

REFERENCES

1. **Ackerley, D. F., C. F. Gonzalez, C. H. Park, R. Blake, M. Keyhan, and A. Matin.** 2004. Chromate-reducing properties of soluble flavoproteins from *Pseudomonas putida* and *Escherichia coli*. Appl. Environ. Microbiol. **70:**873–882.
2. **Ackerley, D. F., C. F. Gonzalez, M. Keyhan, R. Blake, and A. Matin.** 2004. Mechanism of chromate reduction by the *Escherichia coli* protein, NfsA, and the role of different chromate reductases in minimizing oxidative stress during chromate reduction. Environ. Microbiol. **6:**851–860.
3. **Ackerley, D. F., C. F. Gonzalez, M. Keyhan, R. Blake, and A. Matin.** 2005. Biomolecular strategy to decrease chromate toxicity to remediating bacteria, p. 259–268. *In* M. de Conçeicao Cunha and C. A. Brebbia (ed.), Water resources management III. WIT Press, Wessex, England.
4. **Asad, N. R., L. M. Asad, A. B. Silva, I. Felzenszwalb, and A. C. Leitao.** 1998. Hydrogen peroxide effects in *Escherichia coli* cells. Acta Biochim. Pol. **45:** 677–690.
5. **Barceloux, D. G.** 1999. Chromium. J. Toxicol. Clin. Toxicol. **37:**173–194.
6. **Carmel-Harel, O., and G. Storz.** 2000. Roles of the glutathione- and thioredoxin-dependent reduction systems in the *Escherichia coli* and *Saccharomyces cerevisiae* responses to oxidative stress. Annu. Rev. Microbiol. **54:**439–461.
7. **Cervantes, C., J. Campos-Garcia, S. Devars, F. Gutierrez-Corona, H. Loza-Tavera, J. C. Torres-Guzman, and R. Moreno-Sanchez.** 2001. Interactions of chromium with microorganisms and plants. FEMS Microbiol. Rev. **25:**335–347.
8. **Cheung, K. J., V. Badarinarayana, D. W. Selinger, D. Janse, and G. M. Church.** 2003. A microarray-based antibiotic screen identifies a regulatory role for supercoiling in the osmotic stress response of *Escherichia coli*. Genome Res. **13:**206–215.
9. **Das, A., R. Silaghi-Dumitrescu, L. G. Ljungdahl, and D. M. Kurtz, Jr.** 2005. Cytochrome *bd* oxidase, oxidative stress, and dioxygen tolerance of the strictly anaerobic bacterium *Moorella thermoacetica*. J. Bacteriol. **187:**2020–2029.
10. **Drapeau, G. R., F. Gariepy, and M. Boule.** 1984. Regulation and SOS induction of division inhibition in *Escherichia coli* K12. Mol. Gen. Genet. **193:**453–458.
11. **Eichhorn, E., J. R. van der Ploeg, and T. Leisinger.** 1999. Characterization of a two-component alkanesulfonate monooxygenase from *Escherichia coli*. J. Biol. Chem. **274:**26639–26646.
12. **Gonzalez, C. F., D. F. Ackerley, S. V. Lynch, and A. Matin.** 2005. ChrR, a soluble quinone reductase of *Pseudomonas putida* that defends against H_2O_2. J. Biol. Chem. **280:**22590–22595.
13. **Goodgame, D. M., and A. M. Joy.** 1986. Relatively long-lived chromium(V) species are produced by the action of glutathione on carcinogenic chromium(VI). J. Inorg. Biochem. **26:**219–224.
14. **Hansen, A. M., Y. Qiu, N. Yeh, F. R. Blattner, T. Durfee, and D. J. Jin.** 2005. SspA is required for acid resistance in stationary phase by downregulation of H-NS in *Escherichia coli*. Mol. Microbiol. **56:**719–734.
15. **Imlay, J. A., and S. Linn.** 1987. Mutagenesis and stress responses induced in *Escherichia coli* by hydrogen peroxide. J. Bacteriol. **169:**2967–2976.
16. **Kadiiska, M. B., Q. H. Xiang, and R. P. Mason.** 1994. In vivo free radical generation by chromium(VI): an electron resonance spin trapping investigation. Chem. Res. Toxicol. **7:**800–805.
17. **Keyhan, M., D. F. Ackerley, and A. Matin.** 2003. Targets of improvement in bacterial chromate bioremediation, section E-06, p. 143–151. *In* M. Pellei and A. Porta (ed.), Remediation of contaminated sediments. Batelle Press, Columbus, Ohio.
18. **Llagostera, M., S. Garrido, R. Guerrero, and J. Barbe.** 1986. Induction of SOS genes of *Escherichia coli* by chromium compounds. Environ. Mutagen. **8:**571–577.
19. **Lofroth, G., and B. N. Ames.** 1978. Mutagenicity of inorganic compounds in *Salmonella typhimurium*: arsenic, chromium and selenium. Mutat. Res. **53:** 65–66.
20. **Lomovskaya, O., K. Lewis, and A. Matin.** 1995. EmrR is a negative regulator of the *Escherichia coli* multidrug resistance pump EmrAB. J. Bacteriol. **177:**2328–2344.
21. **Lynch, S. V., E. L. Brodie, and A. Matin.** 2004. Role and regulation of σ^S in general resistance conferred by low-shear simulated microgravity in *Escherichia coli*. J. Bacteriol. **186:**8207–8212.
22. **Magnusson, L. U., A. Farewell, and T. Nystrom.** 2005. ppGpp: a global regulator in *Escherichia coli*. Trends Microbiol. **13:**236–242.
23. **Matin, A.** 2001. Stress response in bacteria, p. 3034–3046. *In* G. Bitton (ed.), Encyclopedia of environmental microbiology, vol. 6. John Wiley and Sons, New York, N.Y.
24. **Maurer, L. M., E. Yohannes, S. S. Bondurant, M. Radmacher, and J. L. Slonczewski.** 2005. pH regulates genes for flagellar motility, catabolism, and oxidative stress in *Escherichia coli* K-12. J. Bacteriol. **187:**304–319.
25. **Miller, C., L. E. Thomsen, C. Gaggero, R. Mosseri, H. Ingmer, and S. N. Cohen.** 2004. SOS response induction by beta-lactams and bacterial defense against antibiotic lethality. Science **305:**1629–1631.
26. **Niederhoffer, E. C., C. M. Naranjo, K. L. Bradley, and J. A. Fee.** 1990. Control of *Escherichia coli* superoxide dismutase (*sodA* and *sodB*) genes by the ferric uptake regulation (*fur*) locus. J. Bacteriol. **172:**1930–1938.
27. **O'Farrell, P. H.** 1975. High resolution two-dimensional electrophoresis of proteins. J. Biol. Chem. **250:**4007–4021.
28. **Peterson, C. N., M. J. Mandel, and T. J. Silhavy.** 2005. *Escherichia coli* starvation diets: essential nutrients weigh in distinctly. J. Bacteriol. **187:**7549–7553.
29. **Pinto, R., Q. X. Tang, W. J. Britton, T. S. Leyh, and J. A. Triccas.** 2004. The *Mycobacterium tuberculosis cysD* and *cysNC* genes form a stress-induced operon that encodes a tri-functional sulfate-activating complex. Microbiology **150:**1681–1686.
30. **Richard, F. C., and A. C. M. Bourg.** 1991. Aqueous geochemistry of chromium: a review. Water Res. **25:**807–816.
31. **Sainz, T., J. Perez, J. Villaseca, U. Hernandez, C. Eslava, G. Mendoza, and C. Wacher.** 2005. Survival to different acid challenges and outer membrane protein profiles of pathogenic *Escherichia coli* strains isolated from pozol, a Mexican typical maize fermented food. Int. J. Food Microbiol. **105:**357–367. (First published 16 September 2005; doi:10.1016/j.ijfoodmicro.2005.04.017.)
32. **Shi, X. L., and N. S. Dalal.** 1988. On the mechanism of the chromate reduction by glutathione: ESR evidence for the glutathionyl radical and an isolable Cr(V) intermediate. Biochem. Biophys. Res. Commun. **156:**137–142.
33. **Shi, X. L., and N. S. Dalal.** 1990. NADPH-dependent flavoenzymes catalyze one electron reduction of metal ions and molecular oxygen and generate hydroxyl radicals. FEBS Lett. **276:**189–191.
34. **Singh, J., D. L. Carlisle, D. E. Pritchard, and S. R. Patierno.** 1998. Chromium-induced genotoxicity and apoptosis: relationship to chromium carcinogenesis. Oncol. Rep. **5:**1307–1318.
35. **Sugiyama, M., A. Ando, A. Furuno, N. B. Furlong, T. Hidaka, and R. Ogura.** 1987. Effects of vitamin E, vitamin B2 and selenite on DNA single strand breaks induced by sodium chromate(VI). Cancer Lett. **38:**1–7.
36. **Vasquez, C. C., C. P. Saavedra, C. A. Loyola, M. A. Araya, and S. Pichuantes.** 2001. The product of the *cysK* gene of *Bacillus stearothermophilus* V mediates potassium tellurite resistance in *Escherichia coli*. Curr. Microbiol. **43:**418–423.
37. **Voitkun, V., A. Zhitkovich, and M. Costa.** 1998. Cr(III)-mediated crosslinks of glutathione or amino acids to the DNA phosphate backbone are mutagenic in human cells. Nucleic Acids Res. **26:**2024–2030.
38. **Wang, Y.** 2002. The function of OmpA in *Escherichia coli*. Biochem. Biophys. Res. Commun. **292:**396–401.
39. **Wang, Y. T.** 2000. Microbial reduction of chromate, p. 225-235. In D. R. Lovley (ed.), Environmental microbe-metal interactions. ASM Press, Washington, D.C.
40. **Wells, D. H., and S. R. Long.** 2002. The *Sinorhizobium meliloti* stringent response affects multiple aspects of symbiosis. Mol. Microbiol. **43:**1115–1127.
41. **Wick, L. M., M. Quadroni, and T. Egli.** 2001. Short- and long-term changes in proteome composition and kinetic properties in a culture of *Escherichia coli* during transition from glucose-excess to glucose-limited growth conditions in continuous culture and vice versa. Environ. Microbiol. **3:**588–599.
42. **Woods, J. S., T. J. Kavanagh, J. Corral, A. W. Reese, D. Diaz, and M. E. Ellis.** 1999. The role of glutathione in chronic adaptation to oxidative stress: studies in a normal rat kidney epithelial (NRK52E) cell model of sustained upregulation of glutathione biosynthesis. Toxicol. Appl. Pharmacol. **160:**207–216.
43. **Xiao, H., M. Kalman, K. Ikehara, S. Zemel, G. Glaser, and M. Cashel.** 1991. Residual guanosine 3′,5′-bispyrophosphate synthetic activity of *relA* null mutants can be eliminated by *spoT* null mutations. J. Biol. Chem. **266:**5980–5990.
44. **Ye, J., S. Wang, S. S. Leonard, Y. Sun, L. Butterworth, J. Antonini, M. Ding, Y. Rojanasakul, V. Vallyathan, V. Castranova, and X. Shi.** 1999. Role of reactive oxygen species and p53 in chromium(VI)-induced apoptosis. J. Biol. Chem. **274:**34974–34980.